IOP Conf. Series: Materials Science and Engineering **416** (2018) 012062 doi:10.1088/1757-899X/416/1/012062

Changes in the Mechanical Properties of Ti Samples with TiN and TiN/TiO_2 Coatings Deposited by Different PVD Methods

E Yankov [1*], M P Nikolova[1], D Dechev[2], N Ivanov[2], T Hikov[2], S Valkov[2], V Dimitrova[3], M Yordanov[3], and P Petrov[2]

[1]University of Ruse "A. Kanchev", Dept. of Material Science and Technology, 8 Studentska Str., Bulgaria

[2]Bulgarian Academy of Sciences, Institute of Electronics, 72 Tzarigradsko Chausse Blvd, Sofia, Bulgaria

[3]Technical University of Sofia, Faculty of Engineering and Pedagogy, Sliven, Bulgaria

*Corresponding author: eyankov@uni-ruse.bg

Abstract. The metallic implants represent a major class of the hard tissue replacement materials. In order to enhance the surface properties of the titanium alloys multicomponent coatings containing ceramic phases are employed to improve the tribological performance, corrosion resistance and biocompatibility. The mechanical properties (elastic modulus, necking region, loss of adhesion) of arc PVD TiN and TiN/TiO_2 coatings deposited on unalloyed Ti (99 wt. %) foil were examined by nanoindentation, uniaxial tensile test while applying a new approach - using thermal imaging camera during the test. The hardness of the TiN coating reached values of 9649 MPa and 67 GPa, while that of the TiN/TiO_2 was lowered down to 8774 MPa and 58.5 GPa which low values are closer to that of the cortical bone. The mechanical behavior of TiN/TiO_2 coated material characterized it as a more plastic system indicating a good deformability while the TiN displayed more fragile behavior. There were no signs of loss of adhesion or loss of coating integrity up to maximum load for all tested TiN and TiN/TiO_2 coated samples. The thermal analysis proves that the coated samples show lower thermal conductivity, which is very important for the performance of an endosseous dental implant for example.

1. Introduction

Identifying the mechanical properties of a material is an issue of importance for its specific application. Various technologies are being used in order to enhance the surface characteristics of different materials [1-3]. As technologies develop, different methods are effectively implemented of surface modifications for metals and alloys used in implantology. All of them aim at increasing the biocompatibility and addressing the shortcomings of a particular implant material. Titanium and its alloys are in the scope of many scientific works applying a different kind of coatings [4-8]. The major drawbacks of these orthopedical materials are that they are relatively soft and have poor wear resistance [9]. Up to the present day, the scientists continue to seek for surface modifications that increase the mechanical biocompatibility and in vivo performance of the exogenous material. The ceramic coatings of biocompatible or bioactive materials could successfully enhance both osseointegration and mechanical properties of the surface. Unfortunately, such coatings are fragile and special conditions of deposition and implantation are required. If the coating is fragmented, corrosion and inflammatory processes leading to early explantation may occur. In this respect, the study focuses on the examination of the change of the mechanical properties of PVD deposited TiN after subsequent glow discharge oxidation

that produces the superficial TiO_2 film. The coatings were deposited on 0.1 mm thick Ti foil enabling to assess the change in the mechanical properties by uniaxial tensile test and nanoindentation.

2. Experimental procedures

The substrate material used was Ti foil received in the form of sheets with the following dimensions: 100×300 mm and thickness of t_0 = 0,1 mm. The chemical composition shown in Table 1 was determined by JEOL JXCA-733 Microprobe scanning electron microscope (SEM) equipped with wavelength dispersive spectrometers (WDS).

Table 1. Chemical composition (wt. %) of the substrate material.

Element	Al	V	Mo	Sb	Hf	Pd	Cd	Fe	Ti
Bare Ti	0.11	0.26	0.33	0.12	0.076	0.055	0.019	0.002	Bal.

Samples were cut out from the sheet material in one direction with respect to the rolling one as shown in Figure 1 c. The sheet samples were with the following dimensions: L_o = 50 mm, L_c = 90 mm, L_t = 150 mm and b_0 = 12.5 ± 0.2 mm.

For the cathodic arc deposition of the TiN, a sidewall positioned evaporating system in a cubic vacuum chamber with water-cooled walls was used. The samples were hanged near the center of a clockwise-rotating with a frequency of 0.5 Hz turntable. To ensure the coating stress relaxation and necessary adhesion a very thin pure layer from the target (at 2.5×10^{-1} Pa in Ar atmosphere for 5 min., bias 600 V, 110 A arc current) was applied. The TiN film was made in a pure N_2 atmosphere at 280-290 °C substrate temperature for a time of 60 min., 108 A arc current, bias 250 V and 7.5×10^{-1} Pa pressure in the working chamber. The TiO_2 film was made by glow plasma discharge using the uppermost located sputtering system in the same chamber. A bias voltage of 1340 V (720 mA current) in a pure O_2 atmosphere at a pressure of 6×10^{0} Pa were applied for a deposition time of 240 min. Both layers' thickness (TiN - 2.7 μm, TiO_2 - 0.8 μm) was attained by means of calotest measurements.

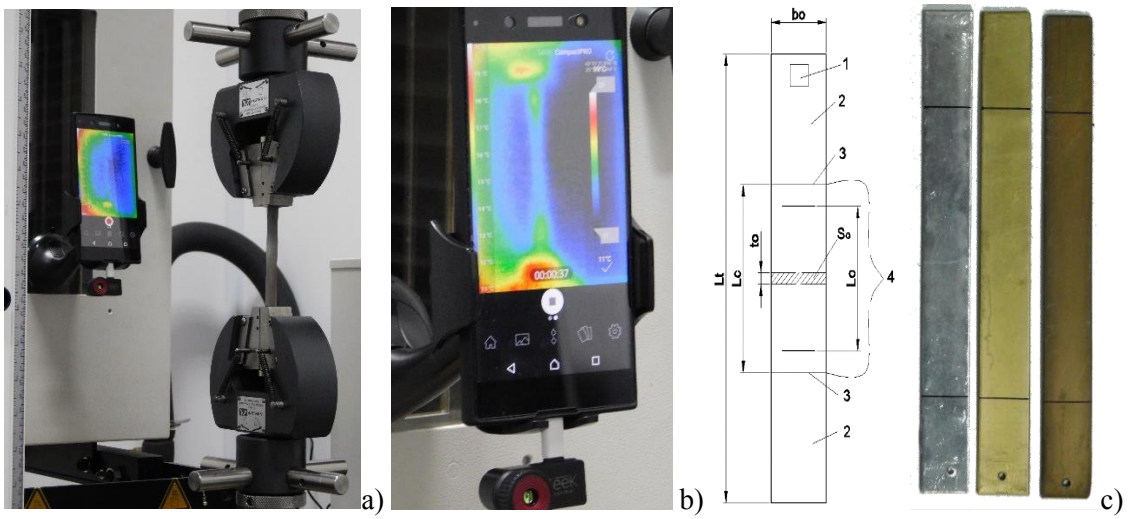

Figure 1. Tensile test equipment and samples: a) universal testing machine; b) SEEK Thermal Compact Pro camera together with the screen and clamp; c) test samples for the uniaxial tensile test (ISO-6892-1:2016) – scheme and appearnce of the uncoated, TiN and TiN/TiO_2 coated samples.

The static uniaxial tensile test was performed on a universal testing machine Instron-3384 (Figure 1a) on the base of the same standard, supplied with a software Bluehill-3. Five of each sample – uncoated, TiN-coated and TiN/TiO_2 coated were examined. For each test control measurements of the working length of testing, height and width were held and the values were set in the used test method via the software program. For the purpose of the testing method, a constant strain rate of 1 mm/min until the load fell down to 300 N and capturing intervals 10 ms of was used. The data were saved in an

appropriate digital form for subsequent analysis. Simultaneously, SEEK Thermal Compact Pro camera with the following characteristics: temperature range – -30 ÷ +330 °C; the size of the thermal sensor - 320x240 pixels, thermal response below 70 mK, spectral range - 7.5÷14 μm, capturing rate - 15 frames per second was used to obtain thermographic images. The thermal camera was equipped with a mobile device with workable software Seek Thermal v.2.1.1.3 (Figure 1 b). The set was adjusted in position to the front of the thermal chamber of the testing machine by a stalk. The camera and machine synchronization were done by joining their software. The real-time monitoring and registration of the thermal fields at the surface of the sample and in the room were obtained during the tensile test. The data collected from the set of thermographic images were used for assessment of the degree of non-uniformity of the thermal field that leads to stresses and deformations occurring in the samples.

The nanohardness values of the TiN and TiN/TiO_2 coating were measured using fine polished Ti foil in order to minimize the surface roughness values. A Vickers nanoindentation tester FISCHERSCOPE H100 using a load force of 20 mN was utilized to determine the Martens hardness HU, plastic hardness H_{pl} and Young's modulus E of the coating. The coating failures were evaluated by JEOL JXCA-733 (Japan) employing accelerating voltage of 19.8 kV.

3. Results and discussions

The values of the coating hardness calculated from the force-depth data of the nanoindentation test are plotted in Table 2. Taking into account the thickness of the coatings, it could be expected that the measured values were influenced by the substrate material used.

Table 2. Hardness values of the TiN and TiN/TiO_2 coating measured with 20 mN load. The abbreviations used stands for HU – universal hardness; H_{pl} - plastic hardness; h – penetration depth, E - Young's modulus, W_{total} – total energy for elastic and plastic deformation, W_r – plastic deformation part of W_{total}

Coating	**HU,** MPa	**H_{pl},** MPa	**h,** μm	**E,** GPa	**W_{total},** nJ	**W_r,** %
TiN	5667±799	9649±4226	0.365±0.06	67±5.1	2.1±1.2	24.7±10.3
TiN/TiO_2	4708±546.8	8774±816.	0.401±0.03	58.5±4.8	6.7±1.8	41±14.8

The oxide deposition on the surface of the nitride resulted in a decrease of hardness and elastic modulus thus closing the mismatch between the bone (E = 9-28.4 GPa [10]) and implant modulus. The nanohardness of arc PVD TiN measured by Hernández L C et al. [11] grown at -300 V bias substrate was higher (17.6 MPa) than the values assessed in the present work. This difference could be attributed to the higher nitrogen content in the gas atmosphere used in the particular study, higher load, the pure Ti substrate material, surface roughness and the resultant coating texture. The universal hardness of the TiN/TiO_2 coating decreased by about 16.92% as opposed to the TiN coated sample. The TiN/TiO_2 plastic hardness reduced by 9.07% on average while the elastic modulus lessened by 12.78 % compared to the TiN coating. These facts imply that the oxidation of the nitride has led to internal stresses' reduction and improvement of plasticity. That is why the total energy for elastic and plastic deformation was increased by 3.2 % after the TiO_2 deposition and simultaneously the plastic deformation part of W_{total} rose up by 66% as opposed to the nitride coating.

After averaging the uniaxial tensile tests results of four tested samples of each kind (uncoated Ti, TiN and TiN/TiO_2 coated), the gathered values were processed and the diagram considered as a representative was the one with the closest mechanical properties to the average results from each indicator diagram. The representative indicator diagrams for the bare Ti, TiN and TiN/TiO_2 coated samples are shown in Figure 2.

For all three samples, because of the smooth transition from elastic to plastic area, the tensile strength at yield had not been established. The absolute extension of the Ti after the TiN deposition significantly reduced its values for the account of an increase in the tensile strength (Figure 2 a). After oxidizing the nitride, a stable downward trend of reducing the tensile strength together with a slight increase in the absolute elongation was observed. Because the applied load and the extension are not additive values, it is not appropriate to be compared. In order to compare the values from the tensile tests, a tensile stress

(σ) – tensile strain (ε) diagram is presented in Figure 2 b. This diagram allows to identify the strength values of the samples - Young's modulus (E), load at the elastic limit (R_e), tensile stress at maximum load (R_m) and tensile stress at tensile strength (σ_u). Additionally, the plasticity characteristics - elongation at tensile strength (ε_m), elongation at break (ε_u) and relative contraction after the break (Z) for the substrate and the coatings were also determined. The calculated values are presented in Table 3.

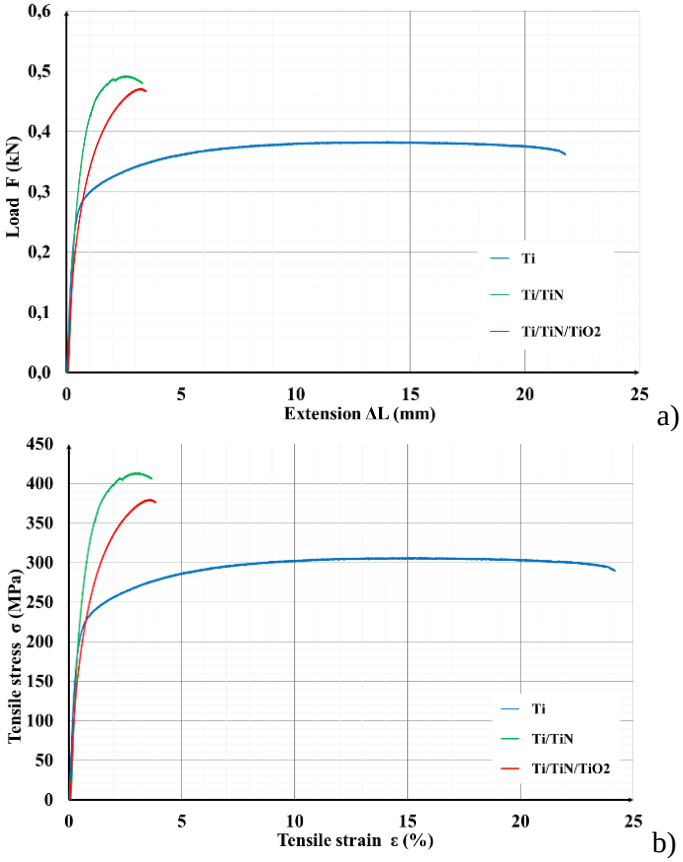

Figure 2. Representative indicator diagrams of: a) extension – applied load, b) tensile stress – tensile strain.

Table 3. Tensile test values of the tested samples: R_e - load at the elastic limit; E - Young's modulus, R_m - tensile stress at maximum load; σ_u - tensile stress at tensile strength; ε_m - elongation at tensile strength; ε_u - elongation at break; Z - relative contraction after the break.

Coating	**R_e ,** MPa	**E,** GPa	**R_m,** MPa	**σ_u,** MPa	**ε_m,** %	**ε_u,** %	**Z,**%
Ti	184.7±5.4	64.1±7.7	306.7±10.6	305.6±10.6	14.6±1.7	14.9±1.9	17.6±3.5
Ti/TiN	227.2±22.1	70.8±12.8	398.5±10.9	398.5±12.2	1.9±0.1.1	1.9±0.4	3.8±0.9
Ti/TiN/TiO_2	154.4±42.2	64.3±17.7	380±13.4	365.5±	2.4±0.5	4.7±0.8	6.1±1.8

The load at the elastic limit for the bare Ti samples showed average values of 184.7 MPa while those coated with TiN indicated higher average values - 227.2 MPa, which were 18.72 % higher than those of the uncoated sample. For the TiN/TiO_2 coated samples, the average load at elastic limit decreased to 154.4 MPa, which means 32.03 % reduction, as opposed to the only nitride coated sample. The results from the load at elastic limit of the coated samples indicate that the elastic strength of the materials lies with the surface film, especially when it has enhanced mechanical properties. The elastic modulus of the Ti foil amounted to about 64.1 GPa and after the TiN deposition it rose up to the average value of 70.8 GPa that means an increase of 9.55 %. After the oxidation, the modulus decreased to 64.3 GPa which was 9.13% less than that of the TiN coating. The decrease in Young's modulus for the TiN/TiO_2

coating points that the oxidized material would have higher toughness against brittle fracture because of the lower internal stresses. The tensile stress at maximum load for the nitride coated sample (R_m - 398,5 MPa) was about 23.04% higher than that of the bare substrate (R_m - 306.9 MPa) for the account of a decrease of plasticity of the TiN (ε_m – 1.86 %) of over 7 times as opposed to the Ti substrate (ε_m – 14.61 %). After oxidation of the coating, the tensile stress at a maximum load slightly decreased (R_m - 380 MPa) with 4.66 % on average. This had a beneficial effect on the plasticity of the TiN/TiO_2 that rose up with 29 % compared to the TiN coated sample. There were no signs of loss of adhesion (de-bonding from the substrate or in between the layers) or loss of coating integrity up to maximum load for all TiN and TiN/TiO_2 coated samples.

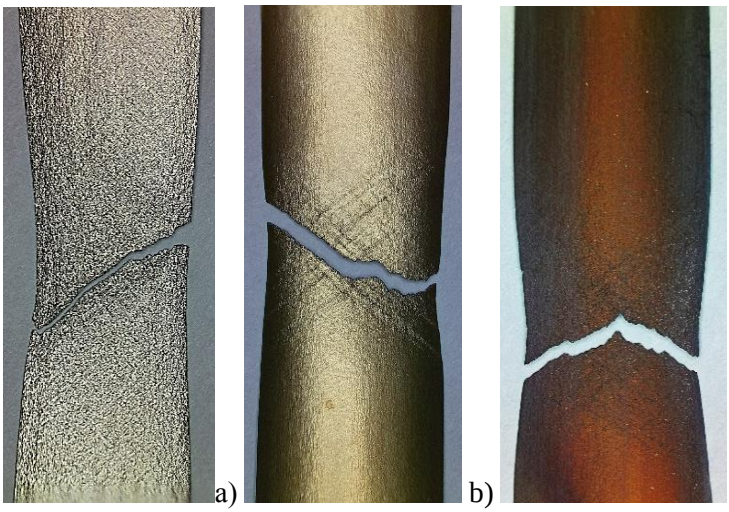

a) b) c)

Figure 3. Macrographs of the tested samples in the ruptured area after the uniaxial tensile test: a) bare Ti foil, b) TiN coated sample, c) TiN/TiO_2 coated sample.

The macrographs of the tested samples in the place of the necking region are presented in Figure 3. Local reorientations and fractures were identified only near the necking region and fractured surfaces. For the coated samples Lüders bands also appeared at the surface. By analogy with the steels, their appearance could be associated with the presence of interstitial N in the Ti substrate because of the diffusion of the element during the deposition process that was characterized by heavy ion bombardment and increased temperature of the substrate material. The strength in the fractures area after the TiN deposition (σ_u – 398.5 MPa) indicated 23.3% higher values as opposed to the bare Ti foil (σ_u – 305.6 MPa). This change was accompanied by lowering the elongation at break with about 8 times (Table 2). After the TiN deposition, the relative contraction after the break (Z – 3,8%) also lessened by 4 times compared to the bare Ti (Z – 17,6%) indicating the ability of the surface to retain the initial geometrical form of the implant if fractures or local effects occur. The oxidized coated samples indicated Z values close to 6.1 %, which were 1.58 times lower than the values of the TiN-coated sample. The mechanical behavior for the TiN/TiO_2 coated material characterized it as a more plastic system (Figure 3.c) compared to the TiN coated samples (Figure 3.b). These results complied with the measured nanoindentation values. The $\varepsilon_u/\varepsilon_m$ for the TiN/TiO_2 coating was equal to 1.94 indicating a good deformability while that ratio for the TiN coated sample amounted 0.998 suggesting more fragile behavior.

The SEM micrographs of the bare Ti sample shown in Figure 4 a, clearly demonstrates the roughening of the surface near the necking zone due to the extensive grains' reorientation. At higher magnification, some sets of twins and slip lines formed by the higher stress in the hexagonal-close packed (hcp) lattice were also seen. The observed grains re-orientation and the inter-crystal changes conform to the higher value of the relative contraction after the break (Z = 17.6%) of the bare Ti. The surface around the necking zone of the coated samples (Figure 4 b and c) looked flatter because of the blocked movements of the crystal lattices by the hard uppermost film and the close interlocking between

their surfaces. Near to the raptured zone, the nitride and oxynitride coatings showed a similar way of cross-section fracturing with respect to the direction of the tensile axis of the PVD films without forming areas with missing parts of the coating. It is clear that the critical load of fracture of the TiN coating is higher than that of the Ti foil. When increasing the applied load after this moment the Ti was being deformed which lead to local contractions mainly in depth than in width (Z = 3.8 %) of the TiN coated sample. The oxidation formed more favorable gains' boundary zones for plastic deformation of the TiN/TiO_2 coating. This fact is evidenced by the increased value of the relative contraction after the break (Z = 6.1 %) suggesting higher plasticity of the coating and more brittle substrate behavior probably because of the higher N diffusion in depth due to the longer deposition process contributing to the very good adhesion. A modern approach evaluating and analyzing the mechanical behavior by thermographic analysis was applied during the uniaxial tensile test.

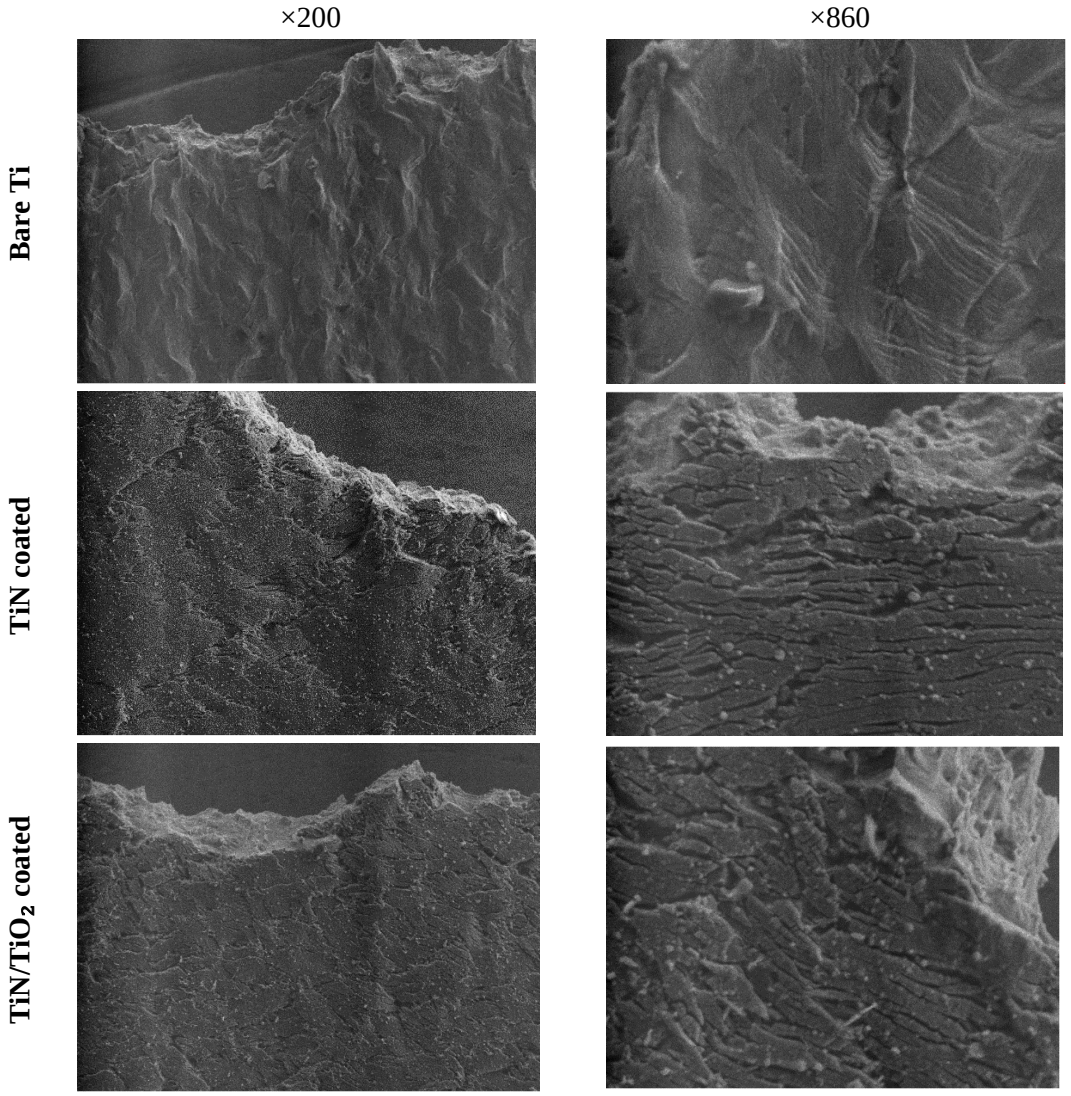

Figure 4. SEM micrographs of the fractures areas after the tensile test at different magnifications.

The thermographic images captured in the beginning (elastic region) and at the end (plastic region and necking area) of the tensile tests of each sample (bare Ti, TiN, and TiN/TiO_2 coated) are shown in Figure 5. The highest was the emitted temperature (27.8 °C) from the bare Ti samples while the lowest one (25.4 °C) was registered for the TiN coated specimen in the elastic area. This fact suggests a hindered heat transfer of the TiN coating and its low plasticity. The emitted temperature in the elastic area from the TiN/TiO_2 coated sample was equal to 26.2 °C implying the enhanced heat transfer and

plasticity as opposed to the TiN coated specimen. All tested samples demonstrated the highest values of emitted temperatures in their elastic regions. After moving into the plastic region, the temperature gradually decreased and that behavior differed from that established for steels. Additionally, the necking zones in all samples occurred in the colder areas of the samples, not in the hotter ones.

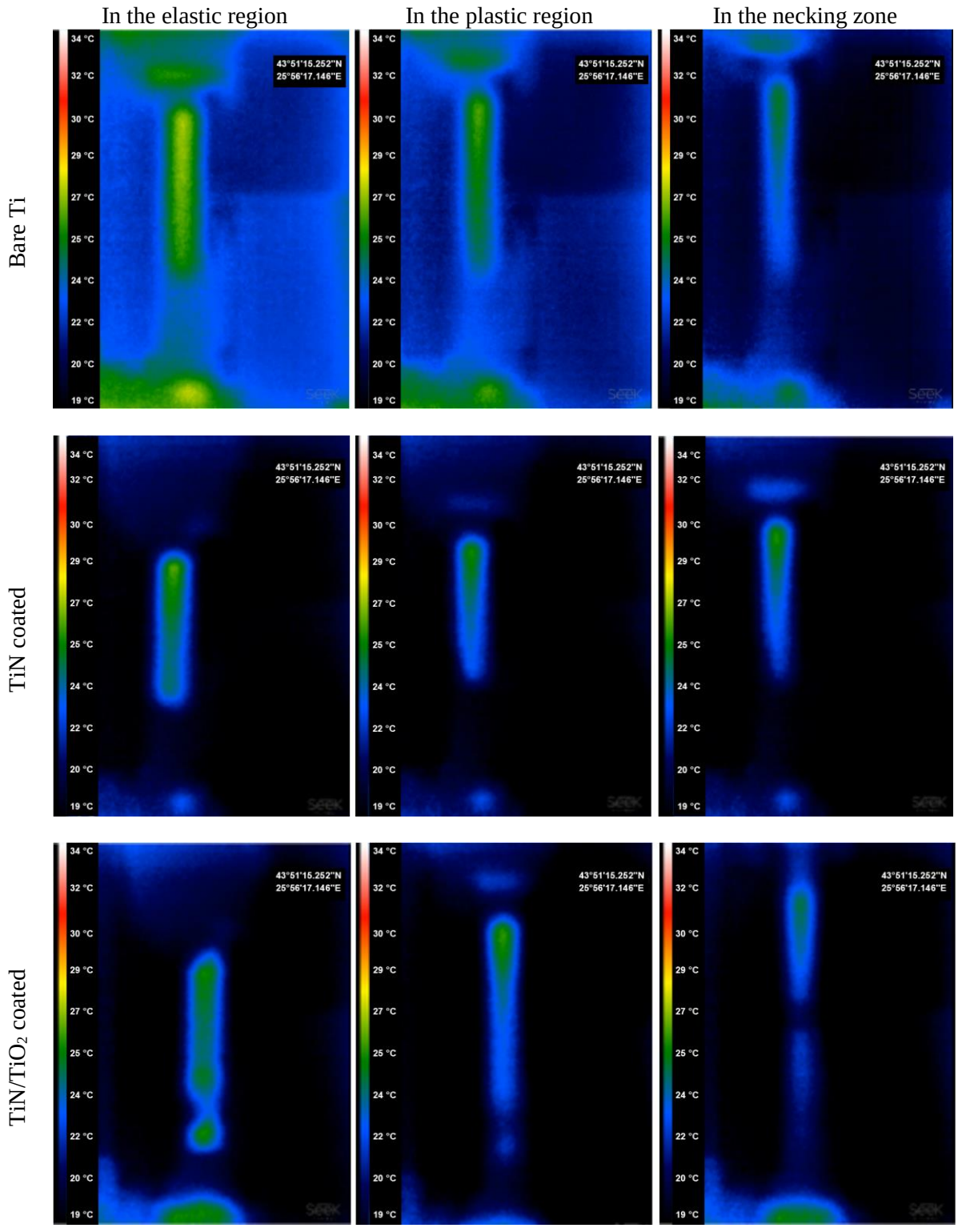

Figure 5. Thermographic images captured during the tensile tests of the bare and coated samples.

4. Conclusions

The deposition of coatings on Ti foil allows for determining different mechanical characteristics of coated systems by using uniaxial tensile test. The method proves to be sensitive to the changes occurring in the mechanical properties of the arc deposited TiN after the glow discharge oxidation when compared to single nitride coating. The decrease in the elastic modulus values after oxidation of the arc deposited TiN coating is an important desirable effect that brings the mechanical properties of the tested system closer to that of the cortical bone. Simultaneously, the plasticity of the TiN/TiO_2 coated sample increases its values with 29% compared to the TiN one at the expense of a small decrease in the hardness and tensile stress at a maximum load. The demonstrated high adhesion strength of the coated systems would prevent the intense fragmentation and separation of parts of the surface film that could trigger inflammatory processes in vivo. The observed differences in the values of the mechanical properties determined by the nanoindentation and tensile tests are dictated by the differences in the tested volumes. The tensile tests results provide an overall outline of the mechanical properties of the tested systems while the nano-hardness results describe the local elastic and plastic behavior of a certain surface area. The thermal analysis proves that the coated samples show lower thermal conductivity, which is a very important fact for the performance of an endosseous dental implant for example.

Additional experiments for determining the changes in the chemical and phase compositions of the coated systems will be needed to explain the differences in the mechanical properties of the tested materials.

5. References

[1] Chawla V, R Jayaganthana and Chandra R 2008 *Mater*. Character. **59** 1015 – 1020
[2] Yan C, Hao L, Hussein A, Wei Q and Shi Y 2017 Microstructural and surface modifications and hydroxyapatite coating of Ti-6Al-4V triply periodic minimal surface lattices fabricated by selective laser melting, *Mater Sci Eng C Mater Biol*. **75** 1515–1524, doi: 10.1016/j.msec.2017.03.066.
[3] Sidambe A T 2014 Biocompatibility of Advanced Manufactured Titanium Implants - A Review *Materials* **7** 8168-8188, doi:10.3390/ma7128168.
[4] Kaluđerović M R, Schreckenbach J P and Graf H-L 2016 Titanium dental implant surfaces obtained by anodic spark deposition – From the past to the future *Materials Science and Engineering C* **69** 1429–1441
[5] Zhang F, Lin L-X, Wang G-W, R Hu, Lin C-J and Chen Y 2012 A high-throughput electrochemical impedance spectroscopy evaluation of bioresponsibility of the titanium microelectrode array integrated with hydroxyapatite and silver, Electrochim. Acta **85** 152– 161
[6] P Mazón, García-Bernal D, Meseguer-Olmoc L, F Cragnolini and De Azad P N 2015 *Ceramics International* **41** 6631–6644
[7] J Kim, W J Lee and Park H W 2016 Mechanical properties and corrosion behavior of the nitriding surface layer of Ti-6Al-7Nb using large pulsed electron beam (LPEB) J Alloys Compd **679** 138-148
[8] Maho A, Detriche S, Delhalle J and Mekhalif Z 2013 *Materials Science and Engineering C* **33** 2686–2697
[9] El-Hadad S, Waly M and Khalifa W 2015 Microstructure evolution and mechanical properties of alpha-beta heat treated Ti-6Al-4V alloy, *22nd Intern. Conf "Advances and Trends in Engineering Materials and their Applications"*, Montreal
[10] Zysset P K 2009 Indentation of bone tissue: a short review, *Osteoporos Int*. **20** 1049–1055
[11] Hernández L, Ponce L, Fundora A, López E and Pérez E 2011 Nanohardness and Residual Stress in TiN Coatings *Materials* **4** 929-940

Acknowledgement

The financial support of this work was provided by the National Science Fund of Ministry of Education and Science, Bulgaria, under Grant project "Gradient functional nanocoatings produced by vacuum technologies for biomedical applications" with number DN 07/3 (2016).